Electronic Supplementary Material

A novel NIR fluorescent probe based on p-mercaptophenylboronic acid -functionalized copper nanoclusters for capmatinib quantification

Ali O Alqarni [a], Rayed Ali A. Alqahtani [a], Ashraf M Mahmoud[a, b], Yahya S. Alqahtani[a], Bassam S.M. Al Kazman[c], Fatmah M. Alshareef [d], Mohamed N. Goda[e], Laila S. Alqarni[e], Ramadan Ali[f], Al-Montaser Bellah H. Ali [b], Mohamed M. El-Wekil[g]

[a] Department of Pharmaceutical Chemistry, Faculty of Pharmacy, Najran University, Najran, Kingdom of Saudi Arabia

[b] Department of Pharmaceutical Analytical Chemistry, Faculty of Pharmacy, Assiut University, Assiut, Egypt.

[c] Department of Pharmacognosy, College of Pharmacy, Najran University, Najran, 66462 Saudi Arabia

[d] Department of Chemistry, Faculty of Science, King Abdulaziz University, P. O. Box 80203, Jeddah 21589, Saudi Arabia

[e] Department of Chemistry, College of Science, Imam Mohammad Ibn Saud Islamic University (IMSIU), Riyadh 11623, Saudi Arabia

[f] Department of Pharmaceutical Chemistry, Faculty of Pharmacy, University of Tabuk, Tabuk 71491, Saudi Arabia

[g] Pharmaceutical Chemistry Department, Faculty of Pharmacy, Badr University in Assiut (BUA), 2014101, Assiut, Egypt

Email: raalqahtani@nu.edu.sa

Fluorescence quantum yield measurements of p-MPBA@CuNCs (X)

Quantum yields (Φ_X) were determined relative to Rhodamine B standard (QY = 95% in ethanol at 420 nm) under identical instrumental settings [1]. To avoid inner-filter effects, sample and reference absorbance values were kept below 0.05 at 420 nm. Emission spectra were integrated over the full fluorescence band (corrected for instrument response), and the following relation was applied:

$$\phi_X = \phi_S \times \frac{F_X}{F_S} \times \frac{A_S}{A_X} \times \frac{\eta_X}{\eta_S}$$

Φ_X represents the quantum yield of p-MPBA@CuNCs, ϕ_S represents the quantum yield of Rhodamine B, F_X is the fluorescence intensity of p-MPBA@CuNCs, F_S is the fluorescence intensity of standard (S, Rhodamine B), A refers to the absorbance value and η refers to the refractive index of the solvent (ethanol). The synthesized p-MPBA@CuNCs were dissolved in distilled water (η = 1.33) and S was dissolved in ethanol (η = 1.33).

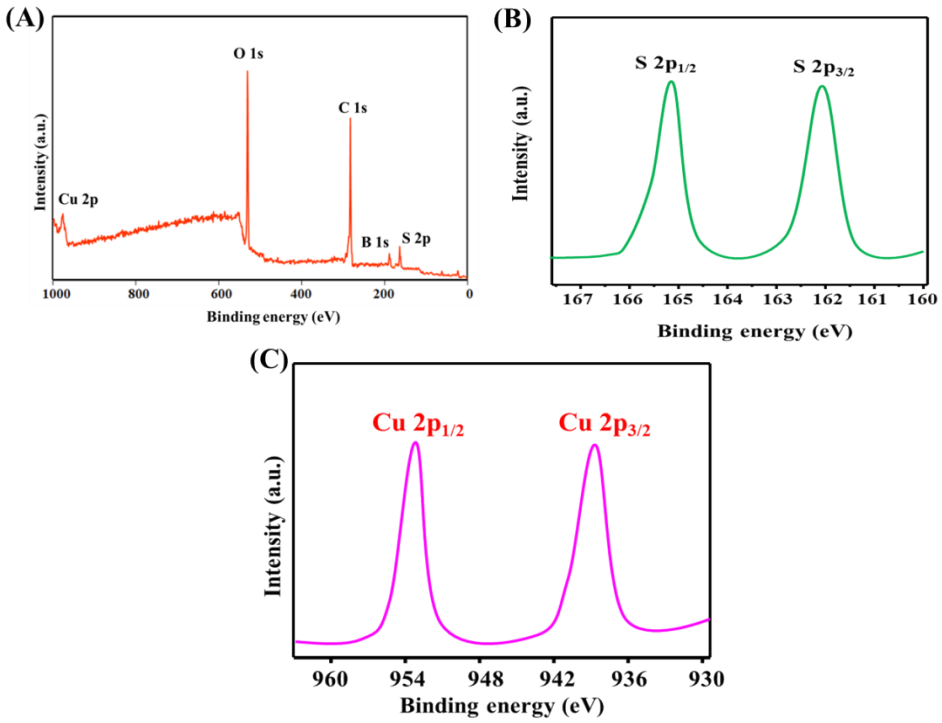

Fig. S1 (A) XPS survey of p-MPBA@CuNCs. Deconvoluted spectra of S 2p (B) and Cu 2p (C).

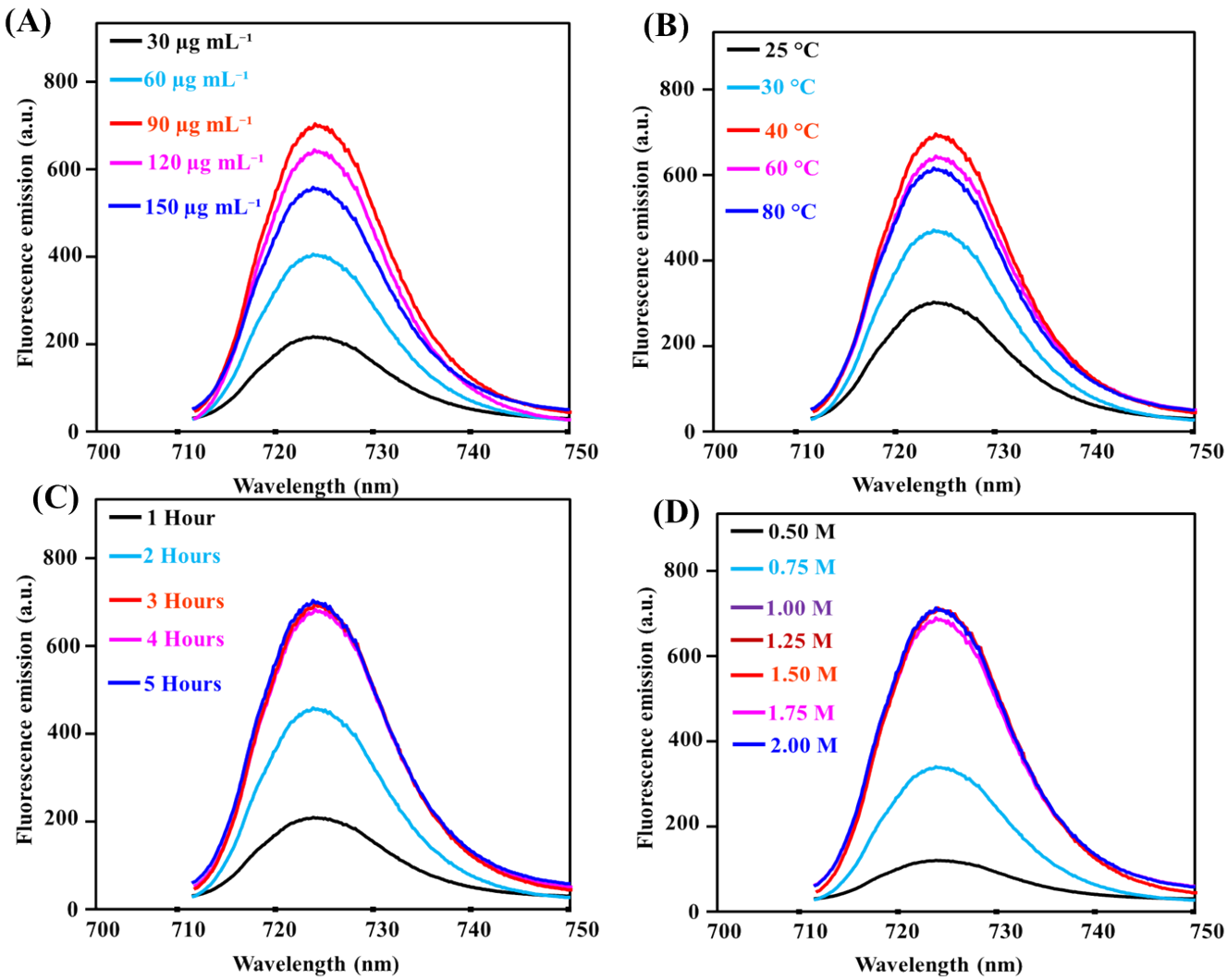

Fig. S2 Effect of synthesis conditions on the fluorescence emission of p-MPBA@CuNCs: (A) Amount of p-MPBA; (B) Synthesis temperature; (C) Synthesis time; (D) Amount of NaOH.

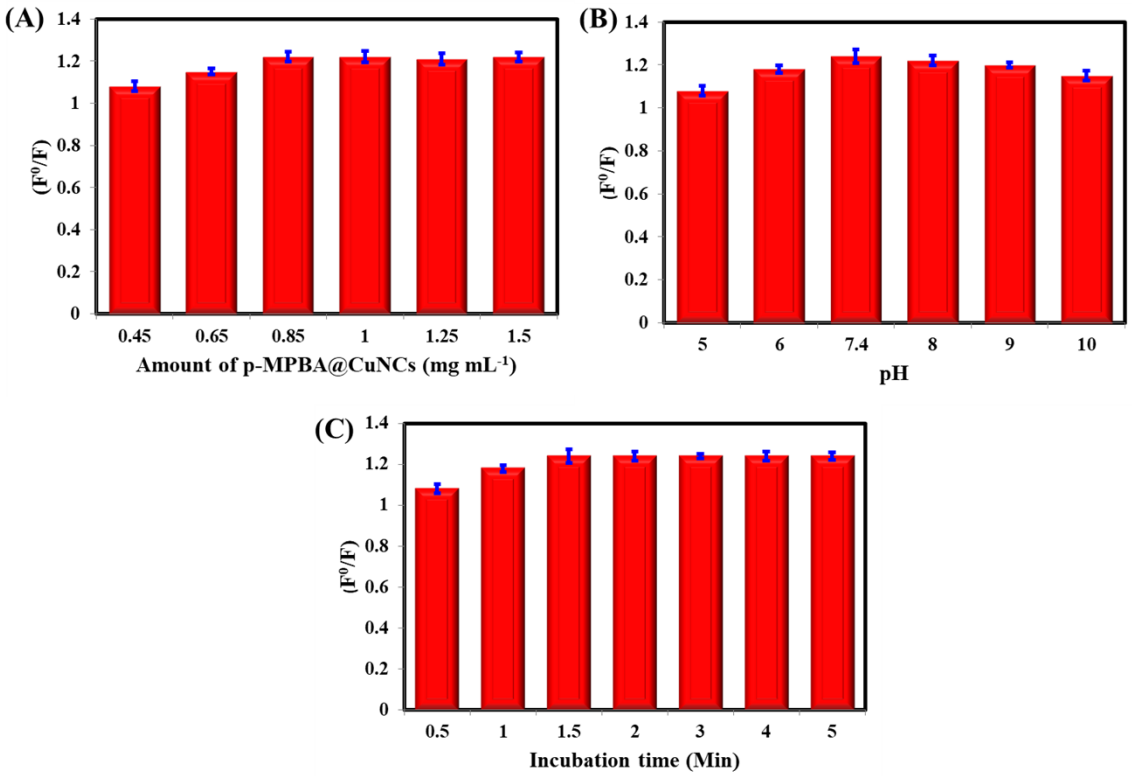

Fig. S3 Effect of detection conditions on the fluorescence quenching of p-MPBA@CuNCs by 20 µM CAMB: (A) p-MPBA@CuNCs dosage, (B) solution pH, and (C) incubation time. Error bars represent the mean ± standard deviation of three independent measurements (n = 3).

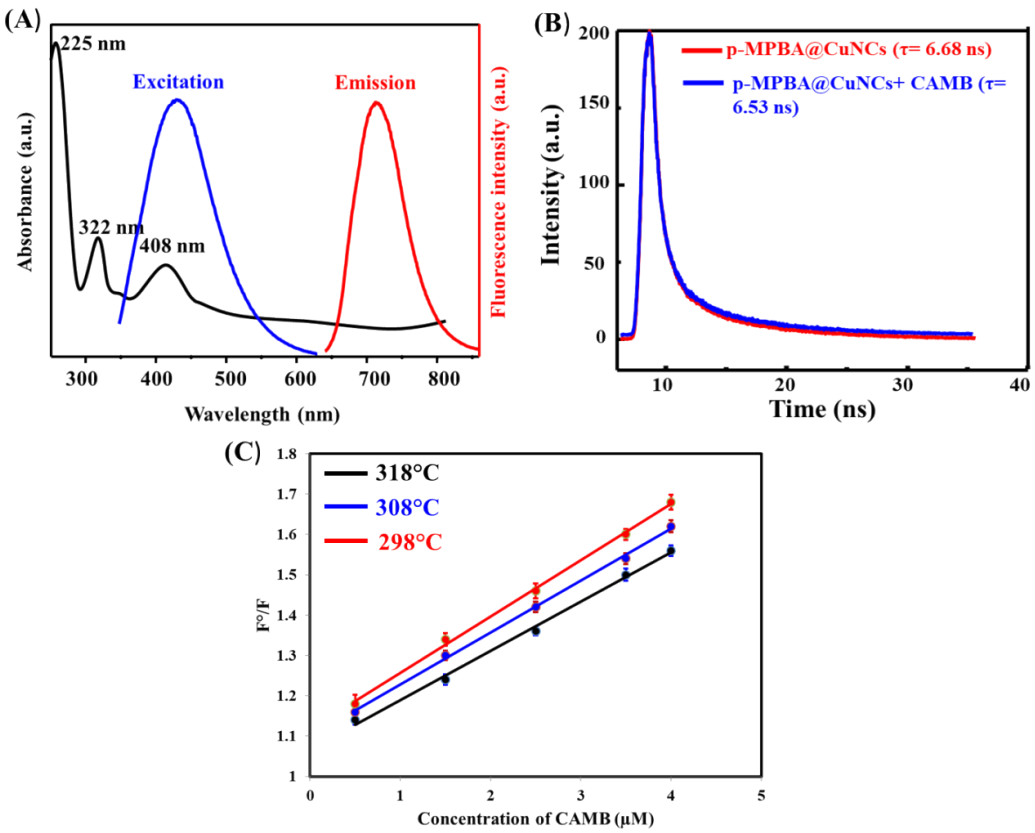

Fig. S4 (A) Spectral overlap between CAMB absorption and p-MPBA@CuNCs excitation/emission profiles. (B) Fluorescence lifetime decay of p-MPBA@CuNCs before and after CAMB addition. (C) Temperature-dependent Stern–Volmer plots (298–318 K) supporting static quenching behavior.

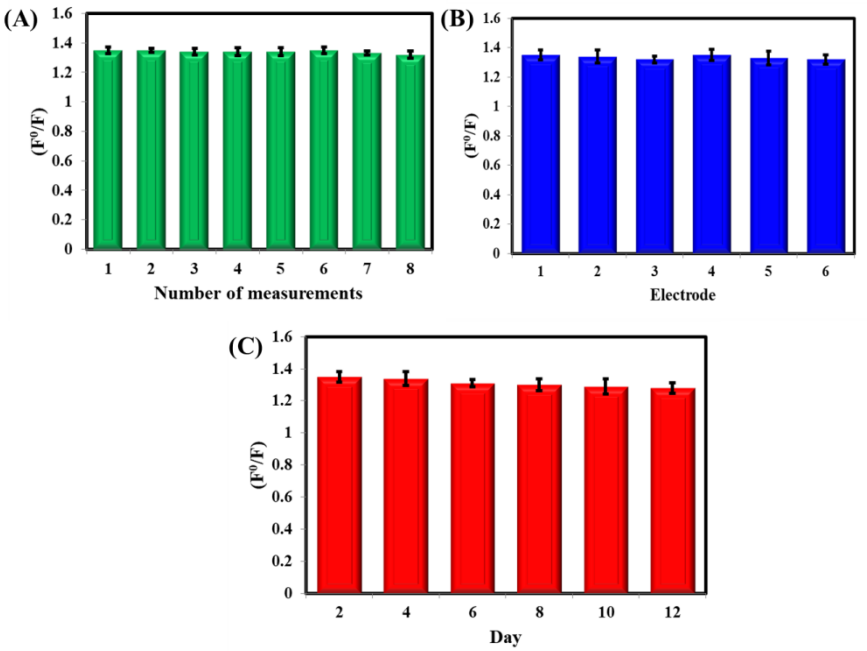

Fig. S5 Repeatbility (A), reproducibility (B), and stability (C) of the p-MPBA@CuNCs for measuring 20 μM CAMB. Each bar represents the average and standard deviation of three replicate measurements.

Table 1 Quantitative parameters of the proposed and reported methods for CMB detection.

Method	Linear range (μM)	LOD (μM)	Cost	Time	Complexity	Interference risk	Reference
HPLC-DAD	0.048-242.7	0.009	High	Slow	High	Moderate	**[2]**
HPLC-FLD	0.05-9.5	------	High	Slow	High	Moderate	**[3]**
UPLC-MS/MS	0.002-7.28	------	Very high	Slow	Very high	Low	**[4]**
Au@PAB/CNFs	0.01-20	0.005	Medium	Moderate	Moderate	Low to Moderate	**[5]**
CeNPs@CNF-CF	------	0.05	Medium	Moderate	Moderate	Low to Moderate	**[6]**
CeNPs@CNF-CF/PGRE	0.005-0.97	0.0014	Medium	Moderate	Moderate	Low to Moderate	**[7]**
Spectrofluorometry	0.04-4.85	0.009	Low	Fast	Simple	High (plasma proteins)	**[2]**
	0-480	0.0036	Low	Fast	Simple	Low to Moderate	**[8]**
	0-370	0.0018	Low	Fast	Simple	Very low	**This work**

References

1. Y. A. Bin Jardan, A. M. Mostafa, J. Barker, A. B. H. Ali, M. M. El-Wekil, A novel route for fabrication of yellow emissive carbon dots for selective and sensitive detection of vitamin B12. Anal. Methods, 17 (2025), pp. 3007-3016.
2. H.M. Ali, A.A. Essawy, I.H. Alsohaimi, A. Nayl, H. Ibrahim, A.-E.-N.-I. Essawy, M. Elmowafy, M. Gamal, Tailoring the photoluminescence of capmatinib towards a novel ultrasensitive spectrofluorimetric and HPLC-DAD monitoring in human serum; investigation of the greenness characteristics. Microchem. J., 181 (2022), Article 107838.
3. A. Zayed, S.A.A. Jaber, J. Al Hroot, S. Hawamdeh, N.M. Ayoub, N.A. Qinna, HPLC with Fluorescence and Photodiode Array Detection for Quantifying Capmatinib in Biological Samples: Application to In Vivo and In Vitro Studies. Molecules, 27 (2022), p. 8582.
4. M. W. Attwa, A. S. Abdelhameed, A. M. Alsibaee, and A. A. Kadi, A Rapid and Sensitive UPLC-MS/MS Method for Quantifying Capmatinib in Human Liver Microsomes: Evaluation of Metabolic Stability by In Silico and In Vitro Analysis. Separations, 10 (2023), **p.** 247.
5. Y. S. Alqahtani, A. M. Mahmoud, B. A. Alyami, M. M. El-Wekil, H. M. Ali, and H. Ibrahim, First electrochemical nanosensor for ultrasensitive quantification of MET inhibitor, capmatinib based on carbon nanofiber networks incorporated with hybrid nanofiller nanogold-loaded porous acetylene black. Microchem. J., 201 (2024), Article 110665.
6. A. Z. Alanazi, K. Alhazzani, M. M. El-Wekil, A. B. H. Ali, M. Darweesh, H. Ibrahim, Sol–gel derived ceramic nanocomposite CNFs anchored with a nanostructured CeO2 modified graphite electrode for monitoring the interaction of a selective tyrosine kinase inhibitor capmatinib with dsDNA. RSC Adv., 14 (2024), pp. 34448-34456.

7. A. Z. Alanazi, K. Alhazzani, M. M. El-Wekil, A. B. H. Ali, M. Darweesh, and H. Ibrahim, A novel disposable ultrasensitive sensor based on nanosized ceria uniformly loaded carbon nanofiber nanoceramic film wrapped on pencil graphite rods for electrocatalytic monitoring of a tyrosine kinase inhibitor capmatinib. Talanta, 279 (2024), Article 126610.
8. M. N. Goda, L. S. Alqarni, H. Ibrahim, A. B. H. Ali, M. M. El-Wekil, Low-energy room-temperature carbon dots for targeted sensing of MET inhibitor capmatinib. RSC Adv., 15 (2025), pp. 28375-28383.